ELSEVIER

Journal of Photochemistry and Photobiology A: Chemistry 144 (2001) 107–117

Journal of Photochemistry and Photobiology A:Chemistry

www.elsevier.com/locate/jphotochem

Energy transfer and optical gain studies of FDS: Rh B dye mixture investigated under cw laser excitation

G.A. Kumar [a], N.V. Unnikrishnan [b,*]

[a] *Optical Materials Group, Centro de Investigaciones en Optica, A.P.I 948, 37000 Leon, Gto, Mexico*
[b] *School of Pure & Applied Physics, Mahatma Gandhi University, Kottayam 686560, Kerala, India*

Received 20 March 2001; received in revised form 20 July 2001; accepted 3 August 2001

Abstract

Radiative and non-radiative (Forster type) energy transfer processes in a dye mixture of FDS and Rh B in methanol under cw Ar ion laser excitation were investigated for fixed donor concentration and varying acceptor concentration. It is found that most of the pump power absorbed by FDS is transferred to Rh B as a useful pump power. Transfer probability (P_{DA}), transfer efficiency both radiative (η_R) and non-radiative (η_{NR}) and optical gain (G) of the system were studied for various pump powers. The gain characteristics of Rh B are found to alter due to the change in the effective fluorescence lifetime caused by energy transfer reaction. Theoretical calculations were also done to find the total transfer efficiency (η_T) at various acceptor concentrations to identify the appropriate energy transfer mechanism responsible for gain enhancement in Rh B. Both radiative and non-radiative transfer processes are taken into consideration in all the calculations. Various energy transfer parameters viz. radiative rate constant (K_R), non-radiative rate constant (K_{NR}), critical concentration (C_0), critical radius (R_0) and half quenching concentration ($[A]_{1/2}$) are calculated by using the Stern–Volmer plots and concentration dependence of radiative and non-radiative transfer efficiencies. Concentration and pump power dependence of the peak gain and lasing wavelengths of the energy transfer dye lasers (ETDL) have also been studied. The experimental results show that the dominant mechanism responsible for the efficient excitation transfer in this mixture is of radiative nature, whereas the long range dipole–dipole (d–d) interaction (Forster type) is comparatively smaller. © 2001 Published by Elsevier Science B.V.

Keywords: Energy transfer; Forster–Dexter theory; Stern–Volmer plot; Optical gain

1. Introduction

The concept of energy transfer in laser dye mixture was studied to improve the efficiency and to broaden the spectral range of dye lasers [1–3]. Energy transfer dye lasers (ETDL) using numerous donor acceptor dye pairs have been reported by various investigators during the last three decades. In 1968, soon after the discovery of organic dye lasers, Peterson and Snavelly [4] demonstrated the feasibility of a dye mixture laser with flash lamp excitation. In 1971, Moller et al. [1] using N_2 laser pumping obtained effective excitation transfer from Rh6G to CV and observed an increase in the power output. A simple theoretical model developed by Dienes [5] was found to be in good agreement with experimental observations for the Rh6G–CV mixture, a dye pair commonly used for most ETDL studies [4–6]. Dienes et al. could explain the variation of gain with acceptor concentration using this theoretical model. Gain measurements done by them on Rh6G–CV mixtures and on CV alone clearly show a higher gain in the mixture as compared to CV alone. This high gain ETDL system was demonstrated in other donor acceptor pairs such as Rh6G: Rh B [7], C30: Rh6G [8], C485: Rh B [9], Uranine: DAMC [10], C440: C485 [11], Rh610: Nile blue [12], C153: TBPR, DCM: TBPR, Nile red: TBPR [13], NB: CC, Rh B: NB [14] Rh6G: Oxazin-4-perchlorate, and Rh B: NB [15]. As a result of this gain enhancement the conversion efficiency of the dye laser was improved considerably. A conversion efficiency of about 200% for the dye mixture Rh6G: Rh B was observed whereas for Rh B alone it was only 7% [7]. It should be noted that dyes like perydine could be made to lase by energy transfer pumping though they do not lase otherwise. This high gain which is the result of an enhanced lifetime of the acceptor [8], produces a blue shift in the emission peak of the acceptor.

Most of the earlier studies on energy transfer have been done using a pulsed laser (N_2 laser) as the excitation source. It was later showed by Panoutsopoulos et al. [12] that the use of an Ar ion laser, which is convenient and widely used pump source, may be practically extended through the use of

* Corresponding author. Tel.: +91-481-597923; fax: +91-481-597731.
E-mail address: spapf@sancharnet.in (N.V. Unnikrishnan).

1010-6030/01/$ – see front matter © 2001 Published by Elsevier Science B.V.
PII: S1010-6030(01)00533-0

energy transfer process to a number of dyes. In this paper, we discuss the excitation energy transfer mechanism of FDS: Rh B dye mixture in methanol using the Ar ion laser excitation.

2. Theoretical considerations

The major role in the redistribution of excitation energy between short wavelength (donor) and long wavelength (acceptor) components played by electron energy transfer may either involve the emission of photons (radiative), or the non-radiative (Forster type). Thus, the two main mechanisms of energy transfer are (1) radiative energy transfer involving the emission of a photon by the donor molecule and its subsequent absorption by the acceptor molecule, and (2) radiationless energy transfer due to the interaction between the donor and acceptor molecule during the excitation lifetime of the donor, prior to its emission of a photon. This mechanism is of two types, i.e. (a) diffusion controlled collision and transfer and (b) resonance transfer due to long range multipole (d–d, d–q or q–q) coupling (Forster type).

Diffusion controlled collision transfer occurs over intermolecular distances of the order of molecular distances. This mechanism is dependent on the solvent viscosity and temperature. Its probability is very small in the concentration range studied [12]. Mechanism (2b) occurs at much greater donor acceptor distances than the collisional diameters. A good overlap of the donor emission spectrum and the acceptor absorption spectrum is required for radiative transfer and resonance transfer due to long range multipole interaction. The radiative energy transfer mechanism (1) is often the dominant mechanism in dilute solution and its occurrence cannot be neglected in studies of radiationless energy transfer. These two mechanisms may also be distinguished by measuring the donor fluorescence lifetime as a function of acceptor concentration, i.e. if the donor lifetime is little affected by the concentration of the acceptor molecule, mechanism (1) can be considered dominant [5].

To understand the quantitative idea of energy transfer mechanism, the kinetic scheme shown in Fig. 1 is made use of. This scheme corresponds to the singlet state of donor and acceptor coupled by an energy transfer rate constant $K_{D\to A}$ to account for transfer from the first excited singlet state (S_1) of the donor to the ground state (S_0) of the acceptor. Each singlet state is pumped with a laser source of intensity I_p at a rate $\sigma_{01}(p)\, I_p$. Lasing occurs in the acceptor molecule at a rate $\sigma_e I_L$, where I_L is the generated laser intensity. Absorption losses at the dye laser frequency are represented by the rate $\sigma_{01}(L)\, I_L$.

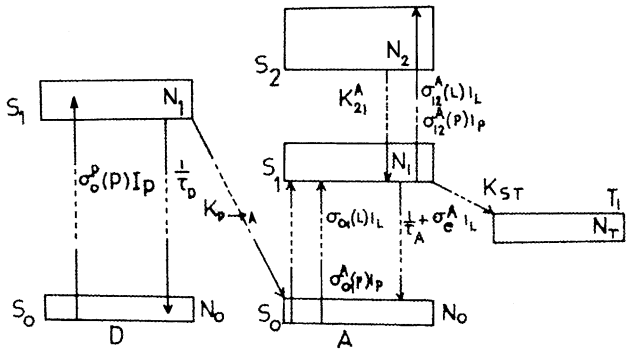

Fig. 1. Kinetic scheme of the ETDL system under cw excitation.

Unlike the case of a pulsed laser pumped ETDL where the triplet state effects are neglected, to develop a gain expression that can be used in the design of a cw ETDL, the triplet state absorption of both the donor and acceptor molecules should be considered. Consequently, the rate equations of the donor–acceptor dye mixture at threshold are given by

$$\frac{dN_{1D}}{dt} = N_{0D}\sigma_D W(t) - K_F N_{1D} N_{0A} - \frac{N_{1D}}{\tau_D} - {}^{D}K_{ST} N_{1D} \tag{1}$$

$$\frac{dN_{1A}}{dt} = N_{0A}\sigma_A W(t) + (K_F + K_R) N_{1D} N_{0A} - \frac{N_{1A}}{\tau_A} - {}^{A}K_{ST} N_{1A} \tag{2}$$

$$N_D = N_{0D} + N_{1D}, \qquad N_A = N_{0A} + N_{1A}, \qquad N = N_A + N_D \tag{3}$$

where N_{0D}, N_{1D}, N_{0A} and N_{1A} indicate the state population densities of the respective states, the subscript 0 and 1 standing for the ground and first singlet states respectively, $W(t)$ (photons $cm^{-2}\, s^{-1}$) is the pump rate, σ_D and σ_A are the absorption cross sections at the pumping wavelength (488 nm) and τ_D and τ_A are the decay times of the singlet states of the donor and acceptor, respectively in the absence of energy transfer. The singlet triplet cross over rate (K_{ST}) is accounted for the total fluorescence lifetime τ_D and τ_A of the donor and acceptor, respectively.

The gain of the dye mixture system at wavelength λ in terms of stimulated and absorption cross section is given by [13]

$$G(\lambda) = \sigma_e^A N_{1A} - \sigma_a^A N_{0A} - N_{TA}\sigma_T^A - N_{0D}\sigma_a^D + \sigma_e^D N_{1D} - \sigma_T^D N_{TD} \tag{4}$$

where σ_T^D and σ_T^A are the triplet state absorption cross section of the donor and acceptor molecules. Since the absorption and emission of the donor molecule can be assumed to be negligibly small in the fluorescence spectrum of the acceptor molecule, the gain coefficient can be written as

$$G(\lambda) = \sigma_e^A N_{1A} - \sigma_a^A N_{0A} - \sigma_T^A N_{TA} - \sigma_T^D N_{TD} \tag{5}$$

The rate Eqs. (1) and (2) can be made dimensionless by multiplying by τ_A/N_A to yield

$$\frac{dn_{1D}}{dx} = n_{0D}\alpha_D - K_F \tau_A n_{1D} n_{0A} N_A - \tau_A \frac{n_{1D}}{\tau_D} - {}^{D}K_{ST}\tau_A n_{1D} \tag{6}$$

$$\frac{dn_{1A}}{dx} = n_{0A}\alpha_A + (K_F + K_R)\tau_A n_{0A} n_{1D} N_A - n_{1A} - {}^{A}K_{ST}\tau_A n_{1A} \quad (7)$$

with

$$x = \frac{t}{\tau_A}, \qquad n_{1D} = \frac{N_{1D}}{N_A}, \qquad n_{0D} = \frac{N_{0D}}{N_A}$$

$$\alpha_D = \sigma_D W(t)\tau_A, \qquad \alpha_A = \sigma_A W(t)\tau_A \quad (8)$$

Since we are measuring the unsaturated gain, ground sate populations are negligibly perturbed. Hence, $N_{0A} = N_A$, i.e.

$$n_{0A} = \frac{N_A}{N_A} = 1, \qquad n_{0D} = \frac{N_D}{N_A} = F = \frac{F_D}{1 - F_D}$$

where

$$F_D = \frac{N_D}{N_A + N_D}$$

Under steady state approximation

$$\frac{dn_{1D}}{dx} = \frac{dn_{1A}}{dx} = 0$$

Hence, the above equations reduce to

$$n_{1A} = \left\{\alpha_A + \frac{F_D}{(1 - F_D)} \frac{(K_F + K_R)N_A\alpha_D}{(K_F N_A + k_D + {}^{D}K_{ST})}\right\} \times \frac{1}{(1 + {}^{A}K_{ST}\tau_A)} \quad (9)$$

where $k_D = 1/\tau_D$ is the natural decay rate of the donor. Thus, the final gain equation of the ETDL under cw excitation becomes

$$G(\lambda) = \sigma_e^A \left\{\left(\frac{\alpha_A/\alpha_D + F_D/(1 - F_D)(K_F + K_R)N_A/(K_F N_A + k_D + {}^{D}K_{ST})}{(1 + K_{ST}\tau_A)}\right)\alpha_D N_A\right\} - \sigma_a^A N_A - \sigma_T^D N_{TD} - \sigma_T^A N_{TD} N_{TA} \quad (10)$$

This expression shows that the gain per acceptor molecule of the mixture is increased with the addition of the donor by a factor

$$\frac{F_D}{(1 - F_D)} \frac{(K_F + K_R)N_A}{(K_F N_A + k_D + {}^{D}K_{ST})} \sigma_e^A \frac{\alpha_D N_A}{(1 + K_{ST}\tau_A)} \quad (11)$$

From Eq. (10), it is clear that $G(\lambda)$ is proportional to the pump power and a plot between the two will be a straight line with the slope given by Eq. (11).

The rate constants for total (K_T) and non-radiative (K_{NR}) energy transfer processes are given by the Stern–Volmer expressions [16,17]

$$\frac{I_{0D}}{I_D} = 1 + K_T\tau_{0D}[A] \quad (12)$$

$$\frac{\phi_{0D}}{\phi_D} = 1 + K_{NR}\tau_{0D}[A] \quad (13)$$

where I_{0D} and I_D are fluorescence intensities of donor in the absence and presence of the acceptor respectively, ϕ_{0D} and ϕ_D the corresponding quantum yields, τ_{0D} the fluorescence lifetime of the donor without acceptor and [A] is the acceptor concentration. Knowing the value of τ_{0D}, K_T and K_{NR} can be directly evaluated from the corresponding Stern–Volmer plots.

The critical transfer radius (R_0), for which energy transfer from the excited donor (D^*) to [A] and emission from D^* are equally probable, is obtained by [14]

$$R_0 = \frac{7.35}{([A]_{1/2})^{1/3}} \quad (14)$$

where $[A]_{1/2}$ is the half-quenching concentration.

According to Forster–Dexter theory [18], R_0 is related with the energy transfer probability P_{DA} as

$$P_{DA} = \frac{1}{\tau_{0D}}\left(\frac{R_0}{R}\right)^s \quad (15)$$

where $s = 6$,8 and 10 for d–d, d–q and q–q interactions, respectively . Also the respective critical radii are defined by the expressions [19]

$$R_0^6 = \frac{3h^4c^4Q_A}{4n^4} \frac{\int f_S(E)F_A(E)\,dE}{E^4} \quad \text{(for d–d interaction)} \quad (16)$$

$$R_0^8 = \frac{135h^9c^{84}Q_A}{4n^4} \frac{\int f_S(E)F_A(E)\,dE}{E^8} \quad \text{(for d–q interaction)} \quad (17)$$

$$R_0^{10} = \frac{225h^{11}c^{104}Q_A}{2n^6} \frac{\int f_S(E)F_A(E)\,dE}{E^{10}} \quad \text{(for q–q interaction)} \quad (18)$$

where $f_S(E)$ is the normalised emission lineshape function of the acceptor, $F_A(E)$ the normalised absorption lineshape function of the acceptor, Q_A the oscillator strength of the absorption band of the acceptor which is in resonance with the donor emission transition and E is the average energy of the overlapping transition.

Total energy transfer efficiency (η_T) is written as the sum of the two parts

$$\eta_T = \eta_R + \eta_{NR} \quad (19)$$

where

$$\eta_R = 1 - \frac{I_D}{I_{0D}} \quad (20)$$

$$\eta_{NR} = 1 - \frac{\phi_D}{\phi_{0D}} \quad (21)$$

For the long-range d–d transfer the above equation can be written as [15]

$$\eta_{NR} = \pi^{1/2} X \exp(X^2)(1 - \text{erf}\, X) \tag{22}$$

where $X = [A]/[A]_0$ is the molar concentration expressed relative to the critical molar concentration of the acceptor,

$$[A]_0 = \frac{3000}{2}\pi^{3/2} N R_0^3$$

$$\text{erf}\, X = \frac{2}{\pi^{1/2}} \int_0^X \exp(-t^2)\, dt$$

An alternative and equivalent expression for η_{NR} is given by

$$\eta_{NR} = 1 - \frac{\tau_0}{\tau_{0D}} \tag{23}$$

The radiative transfer efficiency η_R is obtained by subtracting η_{NR} from η_T using Eq. (19).

The dipole–dipole nature of the non-radiative transfer from D* to [A] can be confirmed by plotting a graph between transfer probability P_{DA} and acceptor concentration [A] on a logarithmic scale. The straight line graph obtained can very well be fitted with the expression [20]

$$\ln P_{DA} = K + \frac{\theta}{3} \ln[A] \tag{24}$$

where $\theta = 6$,8 and10, respectively for d–d, d–q and q–q interactions and P_{DA} is given by

$$P_{DA} = \frac{1}{\tau_{0D}} \left(\frac{I_{0D}}{I_D - 1} \right) \tag{25}$$

where τ_{0D} is given by the well-known Strickler–Berg equation [21]

$$\frac{1}{\tau_{0D}} = 2.88 \times 10^{-9} n^2 \nu^2 \int_{abs} \varepsilon(\nu)\, d\nu \tag{26}$$

where $F(\nu)$ is the fluorescence lineshape function and $\varepsilon(\nu)$ is the molar extinction coefficient.

3. Experimental

The dyes used were laser grade supplied by Exciton Company and the solvent was spectroscopic grade methanol. The excitation source was an Ar ion laser (LICONIX 5000 Series) whose 488 nm line is employed to pump the donor molecule. In all the experiments, donor concentration is kept fixed at 10^{-4} mol l^{-1} whereas the acceptor concentration varies. A transverse pumping configuration and detection geometry was used in the experiment. The dye solution was taken in a quartz cuvette of width 1 cm and the solution is pumped by the laser beam. Fluorescence emission from the solution was focused onto the entrance slit of a 0.2 m concave holographic monochromator (McPherson Model 275) which has a wavelength accuracy of ±0.1 nm. The output of the monochromator was fed to a photomultiplier (Oriel Corp., Model 7068) for detection and finally the emission spectrum was recorded on a chart recorder. All the spectra were recorded with a scanning speed of 1000 Å min^{-1}. Experiments were repeated for different pump intensities, viz. 80, 110, 140 and 170 mW. Optical absorption spectra of the samples were recorded on a Hitachi U 2000 spectrophotometer. All the observations were taken at room temperature.

4. Results and discussion

A typical absorption spectrum of FDS and Rh B corresponding to 10^{-4} mol l^{-1} concentration is presented in Fig. 2 (plots a and b). To confirm the energy transfer process the respective emission spectra are also recorded and plotted along with the absorption spectra. Fig. 2 (plots c and d) represent the respective emission lineshapes. Since, most of the area under the emission spectrum of FDS overlaps with the absorption spectrum of Rh B, energy transfer from FDS to Rh B is definitely possible, the extent depending on the overlapping area which is shown as the shaded region in Fig. 2. Various physical phenomena that are occurring in the dye mixture due to energy transfer and their functional dependence on a number of parameters are described in detail in the following subsections.

4.1. Dependence of peak wavelength (λ_p) of the donor and acceptor on acceptor concentration

Figs. 3(a) and (b) show the dependence of peak emission wavelength of the donor and acceptor on acceptor concentration. All the curves show the same behavior irrespective of the pump intensities. An important observation is that the donor dye always shows a blue shift, whereas the acceptor emission is characterised by an initial blue shift followed by a red shift and blue shift. The average blue shift observed in the donor emission is estimated to be about 38.3 nm,

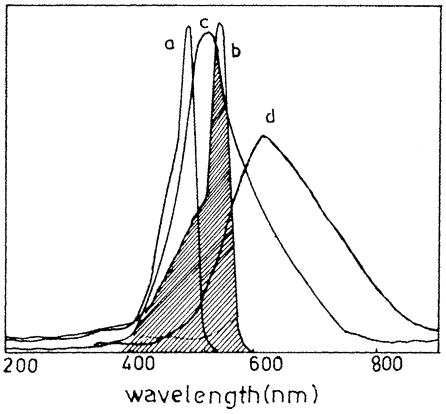

Fig. 2. Spectral characteristics of fluorescence and absorption. Graphs a and b respectively represent the absorption lineshapes of FDS and Rh B dye molecules, c and d represent the corresponding emission lineshapes. The shaded area is the region of energy transfer.

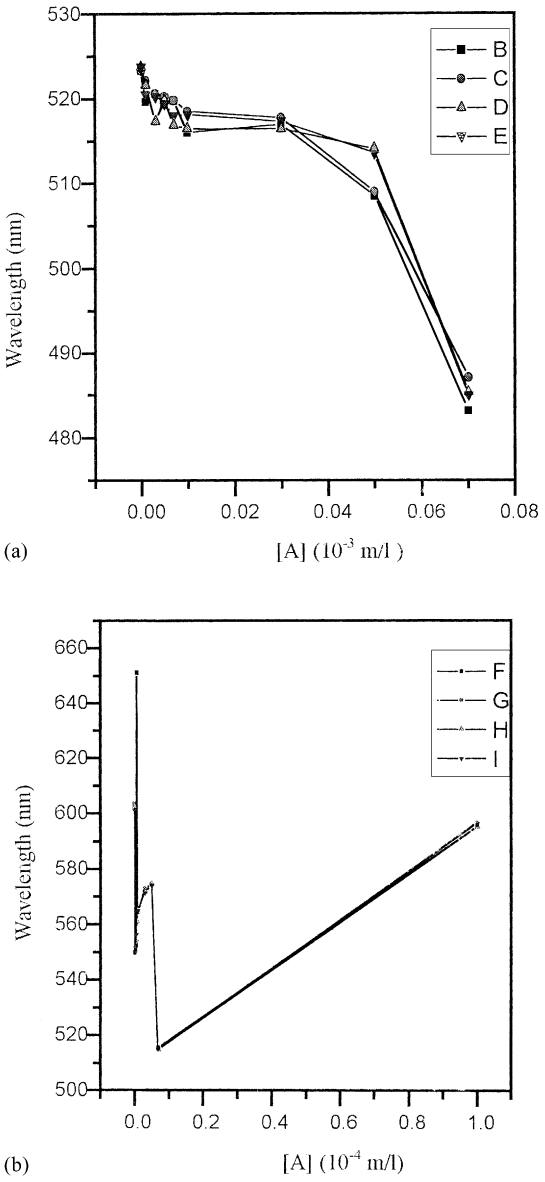

Fig. 3. (a) Dependence of peak emission wavelength of the donor on acceptor concentration (B) 80 mW, (C) 110 mW, (D) 140 mW, (E) 170 mW; (b) dependence of peak emission wavelength of the acceptor on acceptor concentration (F) 80 mW, (G) 110 mW, (H) 140 mW, (I) 170 mW.

whereas for the acceptor emission an initial blue shift of about 57.3 nm (up to 10^{-6} [A] and then a red shift of about 74 nm were observed up to 5×10^{-5} [A]. This is again followed by a blue shift of 59 nm (up to 7×10^{-5} [A]) and a red shift of about 80 nm (up to 10^{-3} [A]). In addition to this, it can also be noticed from Fig. 3 that both these shifts are dependent on the acceptor concentration, where in the case of both the donor as well as the acceptor molecules, shift increases with the acceptor concentration. The blue shift observed in the donor emission can be accounted as follows. As the concentration of the acceptor molecules increases, the intermolecular separation between the donor and acceptor molecules decreases. The collisional heat energy generated in the acceptor system will be sufficient to populate the higher excited singlet state of the donor molecule, which in turn causes the emission to be shifted to the higher energy region. In addition to this being the cw nature of the excitation, some triplet effects should also have some observable contribution in the emission spectrum. The sudden blue shift observed for the acceptor molecule is the result of the energy transfer process. The donor sensitised acceptor system was observed to have a higher gain compared to the unsensitised system due to an increase in the effective lifetime of the acceptor [8]. As a result of this, the gain maximum is shifted towards the blue region [22]. However, the observed blue shift seems to stop at the acceptor concentration 10^{-6} mol l^{-1} and after this a red shift is observed for the acceptor emission up to 5×10^{-5} mol l^{-1} acceptor concentration. This obviates the fact that at higher acceptor concentration ($>7 \times 10^{-5}$ mol l^{-1}) energy transfer effect will not have any dependence on the emission wavelength of the acceptor molecule. In other words, in an ETDL system, above a particular acceptor concentration the acceptor emission wavelength is entirely dependent on its concentration only, i.e. wavelength is shifted to the red region with concentration. This is attributed to the fact that with increase in concentration, both absorption and fluorescence intensities increase resulting in the change of the re-absorption pattern formed by overlapping of absorption and emission spectra. The observed blue shift in the 5×10^{-5} to 7×10^{-5} [A] is tentatively attributed to the thermal energy produced in the mixture which enables more molecules of FDS to be populated in the higher vibrational levels of the first excited singlet state, where from the energy is transferred to the higher vibrational levels of the first excited state of Rh B realising a blue shift. An alternative explanation is that the Rh B is having a more rigid structure as compared to FDS and most of the energy is transferred to Rh B and the Rh B molecules are populated in the higher vibrational levels of the excited singlet state which may also account for the blue shift.

4.2. Dependence of the peak fluorescence intensity (I_L) of the donor and acceptor on acceptor concentration

Figs. 4(a) and (b) show the variation of the emission intensity of the donor and acceptor molecules of the present dye mixture system with the acceptor concentration at various pump powers. All the curves show a sharp reduction in the fluorescence intensity compared with the isolated donor system. At very high acceptor concentration (10^{-4} mol l^{-1}) the donor emission is so weak that it cannot be noticed. This corroborates the fact that the donor system can transfer its energy to the acceptor system non radiatively. However, at the same time radiative type energy transfer will also have exactly the same effect on the donor emission. At very high acceptor concentration, the separation between the donor and acceptor molecule will be so small that effective coupling and thereby energy transfer become possible.

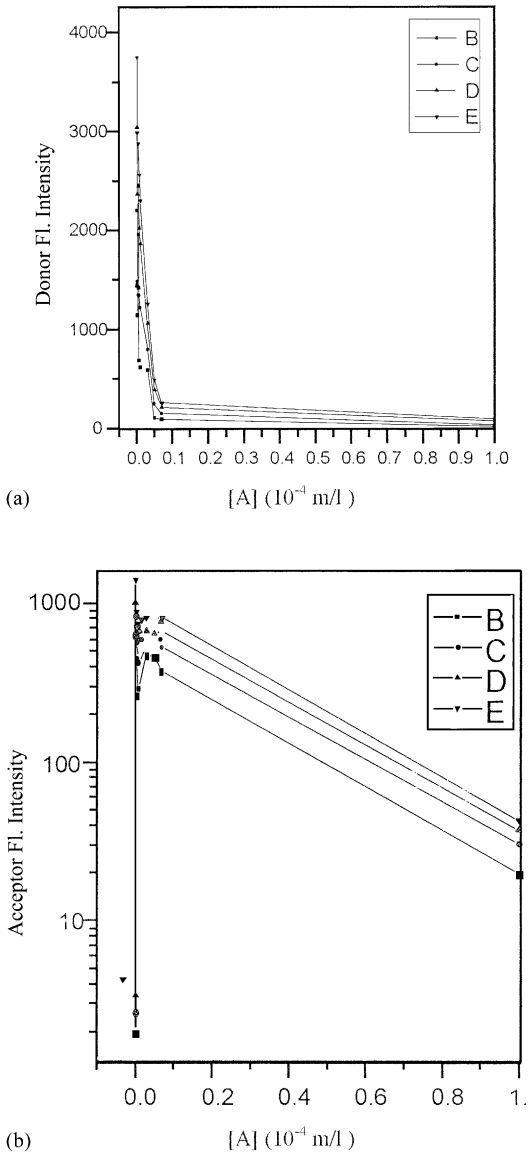

Fig. 4. (a) Dependence of peak emission intensity of the donor on [A] (B) 80 mW, (C) 110 mW, (D) 140 mW, (E) 170 mW; (b) dependence of peak emission intensity of the acceptor on [A] (B) 80 mW, (C) 110 mW, (D) 140 mW, (E) 170 mW.

Another manifestation of the energy transfer process is the increase in the emission intensity of the acceptor molecule as compared to the unsensitised system. It was observed that at lower acceptor concentration (10^{-6} mol l^{-1}) the fluorescence intensity of acceptor was increased on an average by 316 times. Above this concentration and up to 7×10^{-6} mol l^{-1} the acceptor emission shows a reduction in the intensity followed by again an increase of intensity up to 5×10^{-5} mol l^{-1}. At very high acceptor concentration (>7×10^{-5} mol l^{-1}) acceptor emission shows a sharp reduction in intensity due to the self-quenching acceptor–acceptor interaction. The reduction in acceptor emission intensity in the 3×10^{-6} to 7×10^{-6} mol l^{-1} acceptor concentration range is attributed to the re-absorption processes occurring in the acceptor system.

4.3. Pump power dependence on emission intensity

To understand the pump power dependence on the emission intensity and thereby on the efficiency $\varepsilon = (I_{L(max)}/I_p)$, $I_{L(max)}$ of the donor as well as the acceptor emission is plotted for different pump intensities and the variations are

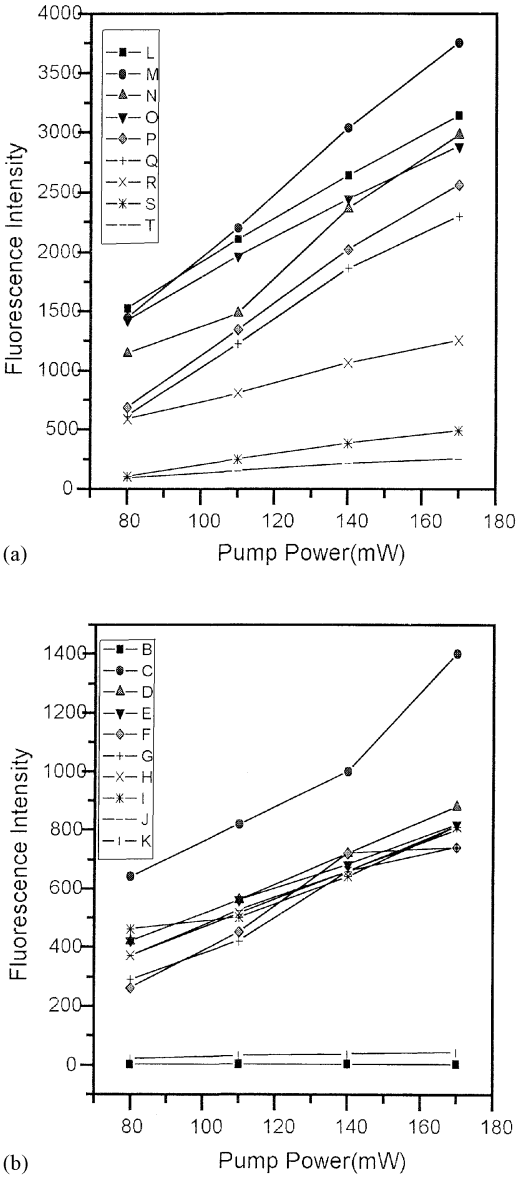

Fig. 5. (a) Pump power dependence of the peak emission intensity of the donor (L) donor only, (M) 10^{-6} mol l^{-1} [A], (N) 3×10^{-6} mol l^{-1} [A], (O) 5×10^{-6} mol l^{-1} [A], (P) 7×10^{-6} mol l^{-1} [A], (Q) 10^{-5} mol l^{-1} [A], (R) 3×10^{-5} mol l^{-1} [A], (S) 5×10^{-5} mol l^{-1} [A], (T) 7×10^{-5} mol l^{-1} [A]; (b) pump power dependence of the peak emission intensity of the acceptor (B) acceptor only, (C) 10^{-6} mol l^{-1} [A], (D) 3×10^{-6} mol l^{-1} [A], (E) 5×10^{-6} mol l^{-1} [A], (F) 7×10^{-6} mol l^{-1} [A], (G) 10^{-5} mol l^{-1} [A], (H) 3×10^{-5} mol l^{-1} [A], (I) 5×10^{-5} mol l^{-1} [A], (J) 7×10^{-5} mol l^{-1} [A], (K) 10^{-4} mol l^{-1} [A].

shown graphically in Figs. 5(a) and (b). In Fig. 5(a) all the plots show almost a linear dependence of $I_{L(max)}$ and hence efficiency upon pump intensity with a noticeable change of slope at higher concentration. In Fig. 5(b), a reduction in the slope is noticed with acceptor concentration showing that there is continuous reduction of the donor efficiency with acceptor concentration. However, for the acceptor the highest efficiency was observed for 10^{-6} mol l^{-1} acceptor concentration and thereafter efficiency is observed to be less than this. Fig. 6 portrays the emission intensity variations of donor and acceptor molecules for different pump powers corresponding to 10^{-4} [D] and 10^{-5} [A].

4.4. Nature of transfer probability function (P_{DA})

The nature of energy transfer process in between donor and acceptor can be studied by evaluating the transfer probability function using Eq. (25) and observing the functional dependence of the transfer provability function on acceptor concentration using Eq. (24). In the present experimental observations, a value of $\theta \sim 6$ is obtained for the ln(P_{DA}) versus ln[A] plot corresponding to the entire acceptor concentration range used in the present study. This confirms the fact that the transfer process is dipole–dipole in nature (Fig. 7).

4.5. Variation of transfer efficiency (η) with acceptor concentration

Energy transfer efficiency (radiative and non-radiative) and rate constants for the present ETDL system in methanol solution have been calculated by studying the relative fluorescence intensities of donor (I_{0D}/I_D) and the relative quantum yield of donor (ϕ_{0D}/ϕ_D) as a function of the acceptor concentration [A] and critical transfer radius R_0. In the presence of acceptor dye, the fluorescence intensity of donor dye is reduced from I_{0D} to I_D by energy transfer to acceptor.

The total transfer efficiency (η_T) was calculated using Eq. (19) at different acceptor concentrations and is shown in Fig. 8 for the d–d process. Non-radiative transfer efficiency

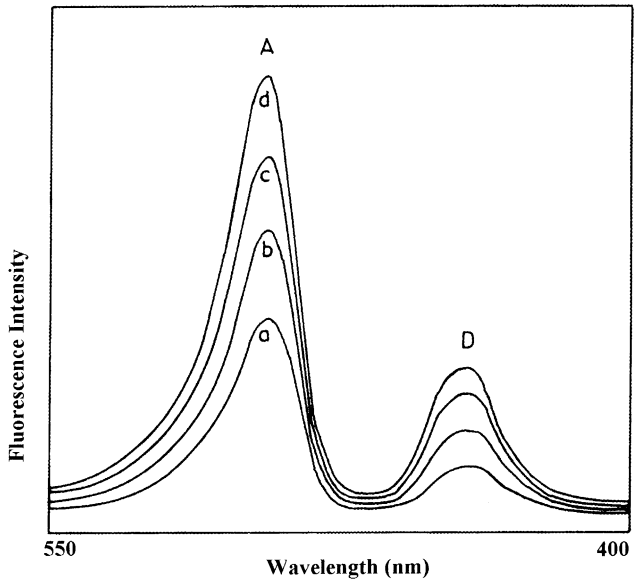

Fig. 6. Emission spectrum of the dye mixture at various pump power with [D] at 10^{-4} mol l^{-1} and [A] at $\times 10^{-5}$ mol l^{-1}.

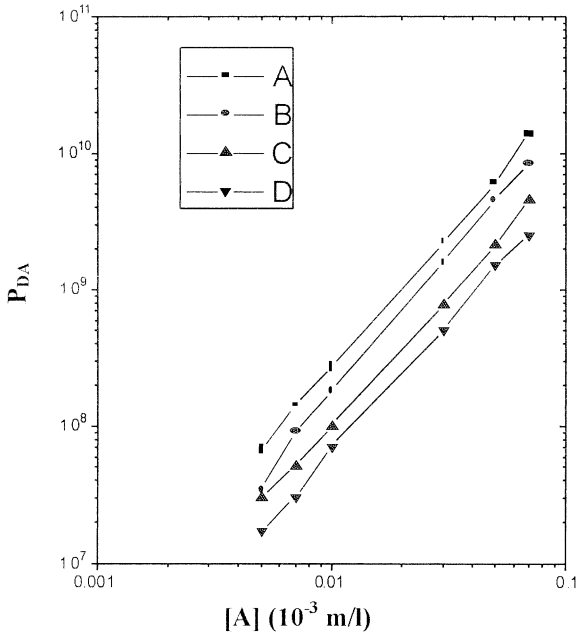

Fig. 7. Dependence of transfer probability on [A] for d–d interaction (A) 80 mW, (B) 110 mW, (C) 140 mW, (D) 170 mW.

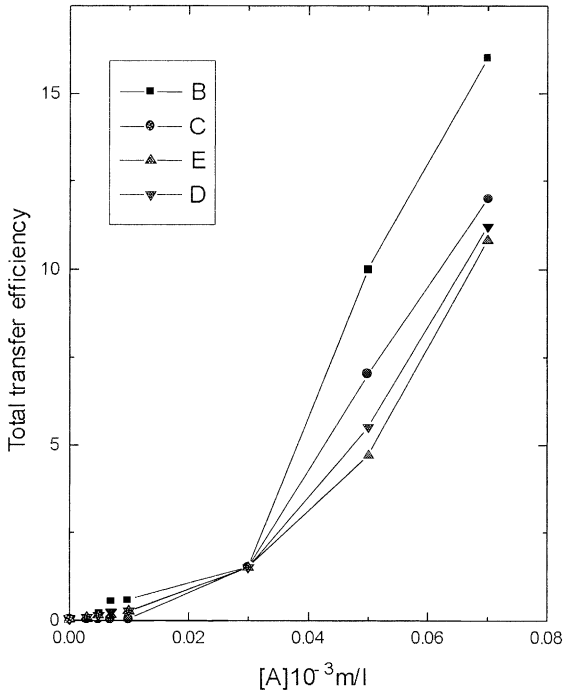

Fig. 8. Dependence of transfer efficiency on [A] for d–d interaction (B) 80 mW, (C) 110 mW, (D) 140 mW, (E) 170 mW.

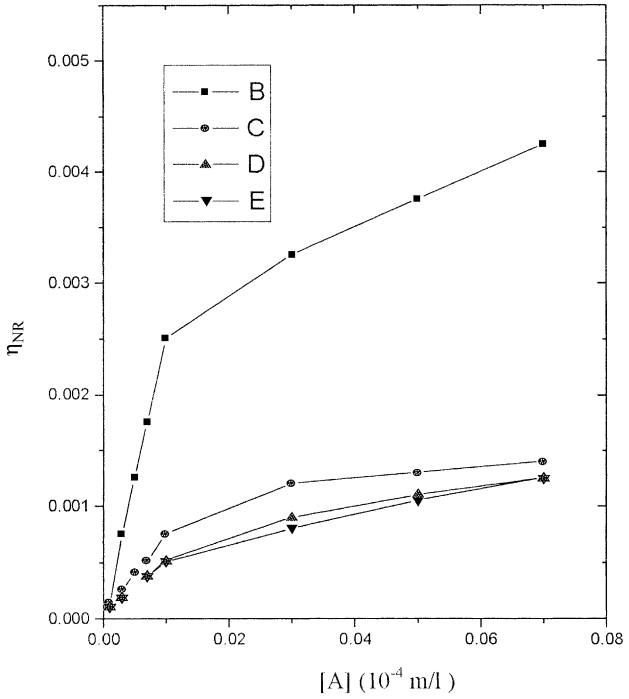

Fig. 9. Dependence of non-radiative transfer efficiency (η_{NR}) on [A] for d–d interaction (B) 80 mW, (C) 110 mW, (D) 140 mW, (E) 170 mW.

(η_{NR}) was calculated using Eq. (22) and is plotted in Fig. 9 for the d–d process. The calculations indicate that both radiative and non-radiative processes are present in the ETDL system consisting of FDS and Rh B in methanol, even though the non-radiative contribution is negligibly small compared to the radiative part. The radiative transfer efficiency is found to have direct dependence on the acceptor concentrations, whereas for the non-radiative transfer efficiency is observed to play its important role at high acceptor concentration ($>0.07 \times 10^{-3}$ mol l^{-1}). The variation of η_R/η_{NR} versus [A] shown in Fig. 10 clearly reveals that at acceptor concentrations $<0.07 \times 10^{-3}$ mol l^{-1} radiative contribution is far exceeding the non-radiative part, whereas at higher acceptor concentrations ($>0.07 \times 10^{-3}$ mol l^{-1}) the radiative contribution will tend to decrease. The pump power dependence of the transfer efficiency (radiative and non-radiative) is graphically shown in Figs. 11(a) and (b). In both the plots, all the curves corresponding to different acceptor concentration show negative slopes indicating that pump power has a negative dependence on the transfer efficiency.

The variation of I_{0D}/I_D versus [A] is always linear in nature as shown in Fig. 12(a). Knowing the value of $[A]_{1/2}$ the half-quenching concentration of the acceptor at which $I_D = I_{0D}/2$ the value of R_0 can be evaluated using Eq. (14). The calculated values of R_0 and $[A]_{1/2}$ for d–d interaction for different pump intensities are tabulated in Table 1. The results clearly show that the value of R_0 is consistent with the d–d type interaction. Results also show an inverse dependence of pump power on critical radius R_0.

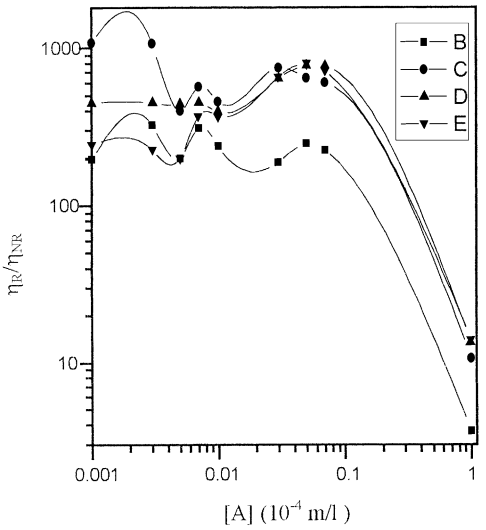

Fig. 10. Plot of η_R/η_{NR} vs. [A] (B) 80 mW, (C) 110 mW, (D) 140 mW, (E) 170 mW.

Also the curves I_{0D}/I_D versus [A] in Fig. 12(a) give the values of $K_T\tau_{0D}$ for different pump powers where $K_T = K_R + K_{NR}$. Again by putting the value of $\tau_{0D} = 6$ ns, the total energy transfer rate constant K_T is calculated for the four pump powers studied. Knowing the values of K_T and K_{NR}, radiative transfer rate K_R can be directly evaluated and the values obtained are collected in Table 1. Observations of these results show that non-radiative transfer due to d–d interaction is comparatively less important than the radiative transfer mechanism in the present ETDL system in the low acceptor concentration range. At high acceptor concentration, a similar tendency was observed (i.e. $K_R > K_{NR}$) whereas the value of K_{NR} observed is comparatively smaller than that of the d–d interaction. In general, both at lower and higher acceptor concentrations radiative transfer process is contributing to the energy transfer mechanism in the present ETDL system. Similarly, by knowing the values of η_{NR} at different acceptor concentrations for different pump powers the value of ϕ_{0D}/ϕ_D can be calculated at various [A] values using Eq. (13) where ϕ_D and ϕ_{0D} are quantum yields of donor molecule with and without acceptor. The variation of ϕ_{0D}/ϕ_D with [A] is also a straight line obeying the Stern–Volmer expression and are shown in Fig. 12(b) for d–d interaction. The slopes ($K_{NR}\tau_{0D}$) directly obtained

Table 1
Calculated radiative parameters of the dye mixture

	Pump power (mW)			
	80	110	140	170
K_R($\times 10^{10}$ s^{-1})	2809	1248	959	919
K_{NR}(d–d) ($\times 10^{10}$ s^{-1})	4.6	1.56	1.24	1.2
R_0(Å)	398.8	284.1	262.7	261.1
$[A]_{1/2}$ ($\times 10^{-5}$ M)	0.626	1.73	2.19	2.23
$W(t)$($\times 10^{20}$) (photons cm^{-2} s^{-1})	1.6	2.74	3.49	4.24

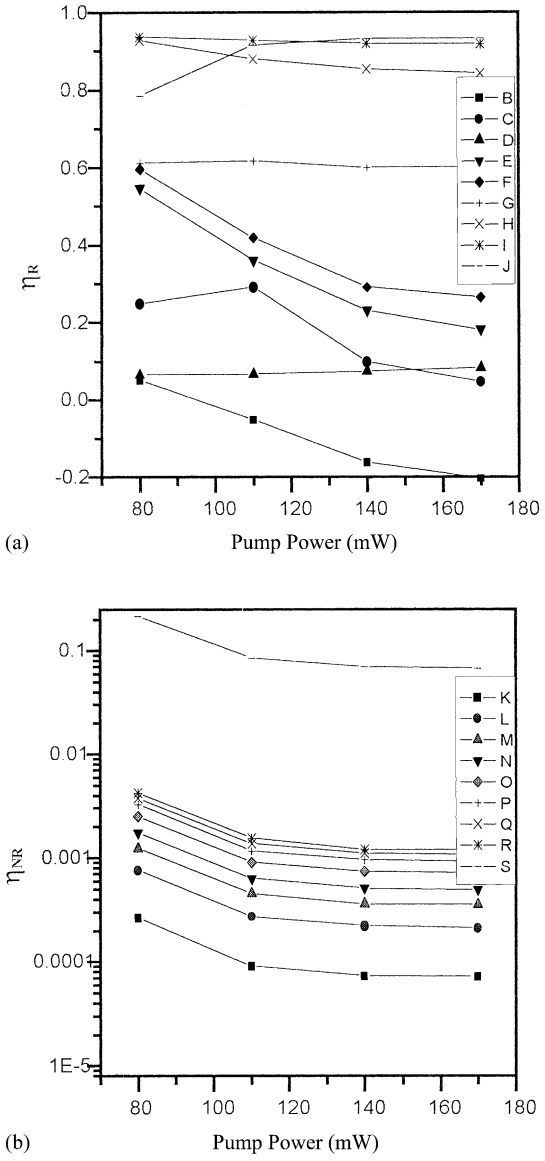

Fig. 11. (a) Dependence of pump power on radiative transfer efficiency (η_R) (B) 10^{-6} mol l^{-1} [A], (C) 3×10^{-6} mol l^{-1} [A], (D) 5×10^{-6} mol l^{-1} [A], (E) 7×10^{-6} mol l^{-1} [A], (F) 10^{-5} mol l^{-1} [A], (G) 3×10^{-5} mol l^{-1} [A], (H) 5×10^{-5} mol l^{-1} [A], (I) 7×10^{-5} mol l^{-1} [A], (J) 10^{-4} mol l^{-1} [A]; (b) dependence of pump power on non-radiative transfer efficiency (η_{NR}) (K) 10^{-6} mol l^{-1} [A], (L) 3×10^{-6} mol l^{-1} [A], (M) 5×10^{-6} mol l^{-1} [A], (N) 7×10^{-6} mol l^{-1} [A], (O) 10^{-5} mol l^{-1} [A], (P) 3×10^{-5} mol l^{-1} [A], (Q) 5×10^{-5} mol l^{-1} [A], (R) 7×10^{-5} mol l^{-1} [A], (S) 10^{-4} mol l^{-1} [A].

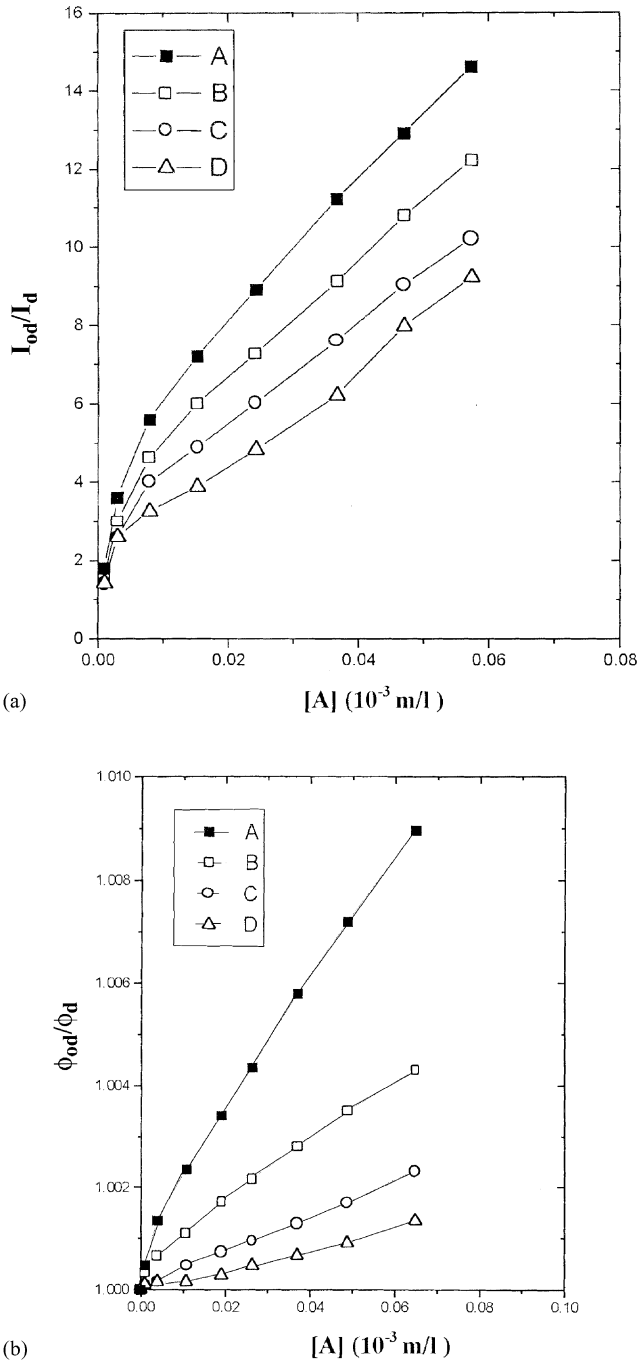

Fig. 12. (a) I_{0D}/I_D vs. [A] plot (Stern–Volmer plot) for [A] $< 0.01\times10^{-3}$ mol l^{-1} (A) 80 mW, (B) 110 mW, (C) 140 mW, (D) 170 mW; (b) ϕ_{0D}/ϕ_D vs. [A] plot (Stern–Volmer plot) for [A] (A) 80 mW, (B) 110 mW, (C) 140 mW, (D) 170 mW.

from the figure corresponding to the four pump powers and assuming the value of τ_{0D} to be ~6 ns, the values of K_{NR} have been calculated and are summarised in Table 1. The pump power dependence of the transfer rate reveals that it is having a negative dependence on the pump power (Fig. 13).

Comparing Eqs. (21) and (23), we can write

$$\frac{\phi_{0D}}{\phi_D} = \frac{\tau_{0D}}{\tau_D} \tag{27}$$

By knowing the values of τ_{0D} and ϕ_{0D}/ϕ_D, the value of τ_D, the fluorescence lifetime of the donor in the presence of acceptor at various acceptor concentrations can be evaluated. The values of τ_D at [A] $= 10^{-3}$ mol l^{-1} are 4.704, 5.49, 5.586 and 5.598 ns for 80, 110, 140 and 170 mW pump powers, respectively.

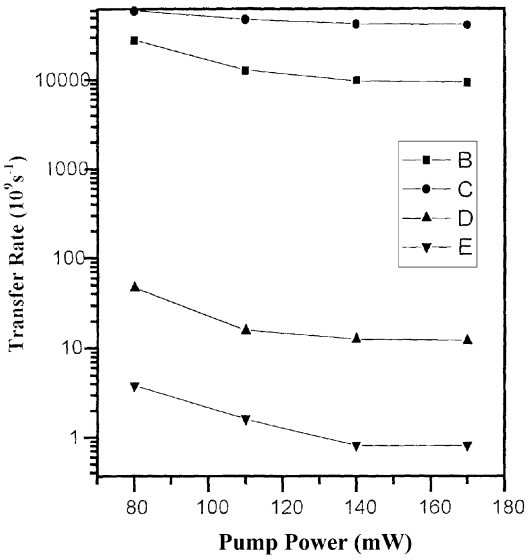

Fig. 13. Variation of the total transfer rate (K_T) with pump power (B) K_R (d–d), (C) K_R (d–d), (D) K_{NR} (d–d), (E) K_{NR} (d–d).

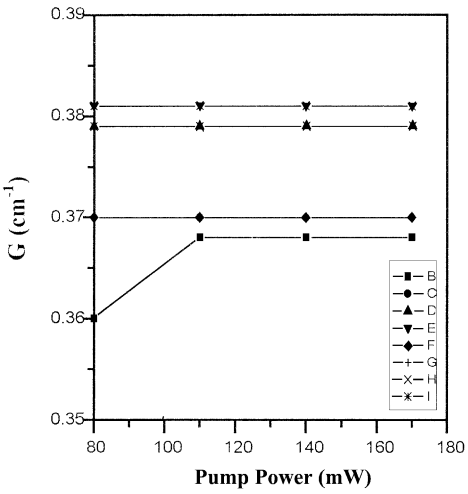

Fig. 15. Dependence of peak gain on pump power in the absence of energy transfer (B) 10^{-6} mol l^{-1} [A], (C) 3×10^{-6} mol l^{-1} [A], (D) 5×10^{-6} mol l^{-1} [A], (E) 7×10^{-6} mol l^{-1} [A], (F) 10^{-5} mol l^{-1} [A], (G) 3×10^{-5} mol l^{-1} [A], (H) 5×10^{-5} mol l^{-1} [A], (I) 7×10^{-5} mol l^{-1} [A].

4.6. Dependence of gain on [A] and pump power

Acceptor concentration and pump power dependence of optical gain $G(\lambda)$ of the acceptor emission is graphically shown in Figs. 14 and 15. Fig. 14 infers that in the absence of energy transfer the gain of the acceptor system varies over a small range of 0.36–0.38 cm^{-1} whereas the pump power has no dependence on the net gain value. Variation of the optical gain with acceptor concentration and pump power after energy transfer process is graphically shown in Figs. 16 and 17. From these figures, it can be noticed that due to the addition of donor, optical gain of the acceptor system is increased many times, the maximum being observed at 0.01×10^{-3} mol l^{-1} acceptor concentration. It was also noticed that at this concentration acceptor gain is increased by 9, 51, 127 and 362 times corresponding to 80, 110, 140 and 170 mW pump powers. Fig. 16 also shows a second gain maximum at 0.05×10^{-3} mol l^{-1} acceptor concentration. Pump power dependence of the optical gain shows that at low acceptor concentration, gain shows almost a saturation effect whereas at high acceptor concentration it shows a linear dependence. The estimated values of the absorption and emission cross sections for various acceptor concentrations are found to be nearly constant except for the numerical factors (Table 2). This justifies the universally ac-

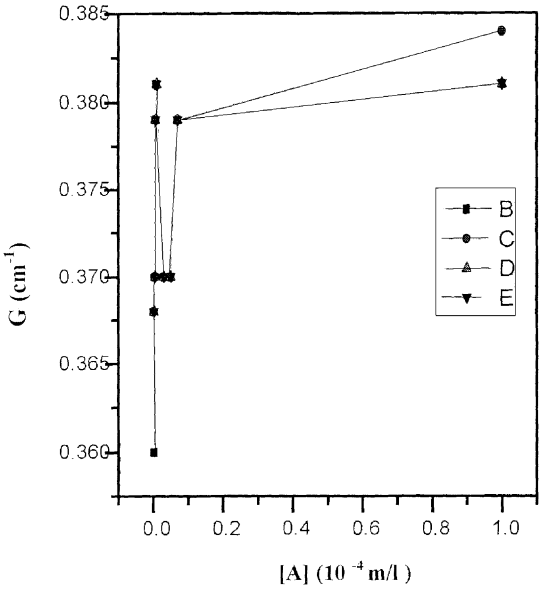

Fig. 14. Dependence of peak gain on [A] in the absence of energy transfer (B) 80 mW, (C) 110 mW, (D) 140 mW, (E) 170 mW.

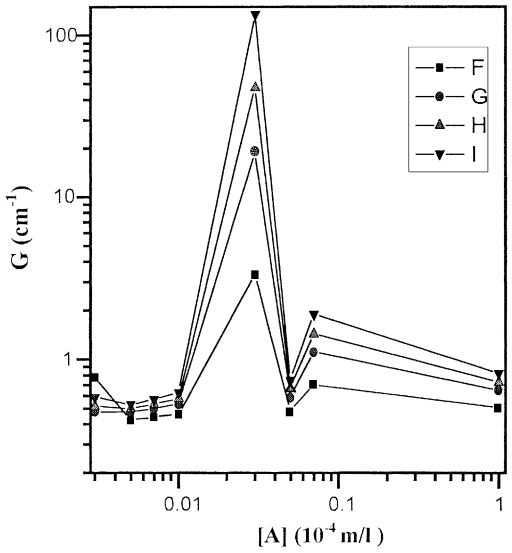

Fig. 16. Dependence of peak gain on [A] in the presence of energy transfer (F) 80 mW, (G) 110 mW, (H) 140 mW, (E) 170 mW.

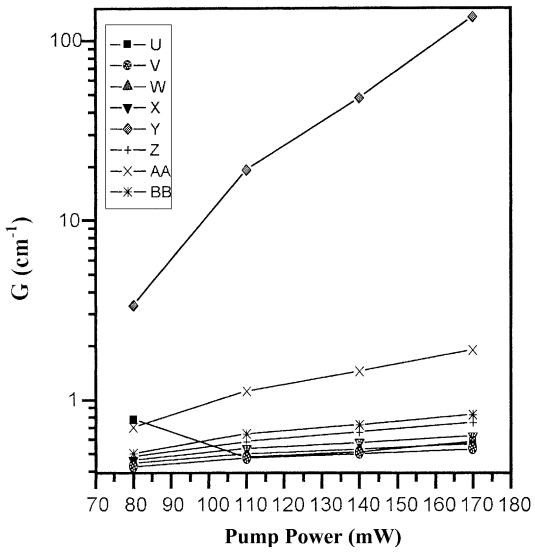

Fig. 17. Dependence of peak gain on pump power in the presence of energy transfer (U) 10^{-6} mol l^{-1} [A], (V) 3×10^{-6} mol l^{-1} [A], (W) 5×10^{-6} mol l [A], (X) 7×10^{-6} mol l^{-1} [A], (Y) 10^{-5} mol l^{-1} [A], (Z) 3×10^{-5} mol l^{-1} [A], (AA) 5×10^{-5} mol l^{-1} [A], (BB) 7×10^{-5} mol l^{-1} [A].

Table 2

Acceptor concentration (10^{-3} mol l^{-1})	Absorption cross section σ_a^A (10^{-19} cm^2)	Emission cross section [a] σ_e^A (10^{-16} cm^2)τ
0.001	4.9	–[b]
0.003	5.5	5.6
0.005	3.6	4.9
0.007	3.9	5.5
0.01	5.1	6.8
0.03	5.4	6.2
0.05	3.3	4.6
0.07	4.8	5.8
0.1	4.2	6.6

[a] $\sigma_e^A = \lambda^4/8\pi cn^2\tau\Delta\lambda_{eff}$, $\tau_{0D} = 6$ ns, $\tau_A = 2.3$ ns, $\sigma_D = 1.6 \times 10^{-20}$ cm^2.

[b] Emission is not prominent.

cepted fact that these cross sections are molecular properties and do not depend on concentration.

5. Conclusions

We have analysed in detail the energy transfer process between FDS and Rh B dye mixture in methanol. We recognise that our results could forecast suitable concentration regions for the wavelength shifts with the acceptor concentration for the dye mixture. Concentration dependence of the acceptor on the energy transfer clearly shows that radiative transfer process is having the major contribution in the present ETDL system, in the entire range of acceptor concentration used. It was also noticed that non-radiative transfer is mainly due to the Forster type d–d interaction. Analysis also shows that the optical gain of the acceptor dye can be increased several times due to the energy transfer process. Optical gain is also observed to have a direct dependence on the pump power.

Acknowledgements

Authors are grateful to the referees for their critical comments and useful suggestions.

References

[1] C.E. Moller, C.M. Verber, A.H. Adelman, Appl. Phys. Lett. 13 (1971) 278.
[2] S.A. Ahmed, J.S. Gergerly, J. Chem. Phys. 61 (1974) 1584.
[3] E.G. Marason, Opt. Commun. 40 (1982) 212.
[4] O.G. Peterson, B.B. Snavelly, Bull. Am. Phys. Soc. 13 (1968) 397.
[5] A. Dienes, M. Madden, J. Appl. Phys. 44 (1973) 4161.
[6] C. Lin, A. Dienes, J. Appl. Phys. 44 (1973) 5050.
[7] P.J. Sebastian, K. Sathyanandan, Opt. Commun. 35 (1980) 113.
[8] T. Urisu, K. Kajiyama, J. Appl. Phys. 47 (1976) 3563.
[9] D. Mohan, S. Sanghi, R.D. Singh, K. Mahendiratta, A. Gaur, J. Photochem. Photobiol. A: Chem 68 (1992) 77.
[10] T. Govindanunni, B.M. Sivaram, J. Lumin. 21 (1980) 397.
[11] L. Thareja, K. Sharma, R.D. Singh, Opt. Commun. 26 (1978) 81.
[12] B. Panoutsopoulos, M. Ali, S.A. Ahmed, Appl. Opt. 31 (1992) 1213.
[13] S. Kohtani, M. Murata, M. Itoh, Chem. Phys. Lett. 22 (1995) 293.
[14] S. Muto, H. Nagashima, K. Nakamura, C. Ito, Electron. Commun. Jpn. 67 (1989) 866.
[15] P.V. Lu, Z.X. Yu, R.R. Alfano, J.I. Gersten, Phys. Rev. A 26 (1982) 3610.
[16] N.J. Turro, Molecular Photochemistry, Benjamin, New York, 1967.
[17] Th. Forster, Ann. Physik. 2 (1948) 55.
[18] D.L. Dexter, J. Chem. Phys. 21 (1953) 836.
[19] G.A. Kumar, P.K. Gupta, N.V. Unnikrishnan, J. Non-Cryst. Solids 275 (2000) 93.
[20] G.A. Kumar, N.V. Unnikrishnan, Solid State Commun. 1049 (1997) 29.
[21] S.J. Strickler, R.A. Berg, J. Chem. Phys. 37 (1962) 814.
[22] T. Urisu, K. Kajiyama, J. Appl. Phys. 47 (1976) 3559.